



Terahertz Plasmon Excitation by Nonlinear Mixing of Two Laser Beams in Graphene Sheet

Neha Verma¹ · Anil Govindan¹ · Pawan Kumar² 

Received: 13 July 2020 / Accepted: 13 October 2020 / Published online: 20 November 2020
© Springer Science+Business Media, LLC, part of Springer Nature 2020

Abstract

Graphene is a promising material for terahertz radiation generation and has unique properties. In graphene, surface plasmon resonance (SPR) can be tuned in THz range in graphene by doping. Here we proposed a scheme of THz graphene plasmon (GP) excitation at difference frequency in graphene sheet by nonlinear mixing of two laser beams. Two laser beams that are obliquely incident, from the free space on the graphene sheet, are deposited on a dielectric substrate. These laser beams impart oscillatory velocities to electrons and exert a difference frequency ponderomotive force on the free electrons of the graphene film, the latter beats with the carrier density to produce a nonlinear current that excite THz SPs at difference frequency. The amplitude of THz graphene SPs falls monotonically because at higher frequency the coupling of SPs is weak.

Keywords Plasmonics · Graphene · Terahertz plasmonics

Introduction

Graphene has become the most fascinating research area in science and technology in present days because of its several unique properties [1–3] and potential applications [4–7]. One important property of graphene is that all its Dirac electrons, irrespective of their energy, have same speed, as energy versus momentum relation is linear. Graphene localizes electron motion in a plane with very small electron effective mass giving rise to high in-plane conductivity. The special spectrum of the charge carriers leads to a number of interesting transport properties.

In many cases it is desirable to tightly confine the probing radiation like as surface plasmons (SPs). SPs are guided electromagnetic modes, propagate along the surface between a conductor and a dielectric or conductor and air with their field amplitude peaking at the interface and falling off exponentially away from it in either medium [8–11]. It also has

been shown that in a noble metal film, SPs can be used to generate light radiation [12].

Moreover, graphene surface plasmons (GPs) have many advantages over metal film SPPs because the conductivity and permittivity of graphene can be controlled by adjusting external gate voltage, chemical doping, etc. The graphene GPs have the properties of extremely high confinement and low Ohmic loss because of their high carrier mobility at room temperature [13–15]. The 2D nature of graphene also gives rise to plasmons with wavelengths that are substantially smaller than free-space electromagnetic radiation of the same frequency by approximately two orders of magnitude, generating large non-local effects. Graphene plasmon is used for making the radiation source with two infrared–visible–ultraviolet range, by using low-energy electrons that may conceivably be generated in an on-chip device [16].

The difference frequency generation (DFG) at mid-infrared in graphene is enhanced due to the presence of plasmon resonance [17–19]. Such an all-optical coupling scheme for plasmon generation in graphene holds great promise, for example, in the design of plasmon sensors or new THz sources. The generation of THz SPs via the nonlinear mixing of lasers in planar structure comprises a dielectric plate coated on top with an ultrathin metal film with suitable ripple is also studied [16]. The metal has larger loss and low confinement of SPs due to low carrier mobilities, surface roughness, grain microstructure

✉ Pawan Kumar
kumarpawan_30@yahoo.co.in

¹ Department of Physics, MMH College Ghaziabad, UP, Ghaziabad, India

² Department of Physics, Research Centre for Compact Radiation Sources, Raj Kumar Goel Institute of Technology, Ghaziabad, UP 201003, India

and impurities [20], and the large electronic density of states compared with GPs at THz frequencies [13, 14].

The most important topics in graphene applications is to generate terahertz (THz) radiation, for that the plasmon frequency in graphene lies in the 1–50 THz frequency regime²¹. The coherent and tunable THz radiation can be generated from SPs excited by a moving electron beam atop multilayer graphene deposited on a substrate [21]. Various approaches have been proposed and investigated to generate THz radiation [22, 23]. However, developing high powered and tunable THz radiation sources remains a significant challenge. Several works demonstrated that graphene plasmonics could be a promising candidate for developing coherent and tunable THz sources with high power density.

In this paper, we proposed a scheme of THz SP generation via the nonlinear mixing of lasers in the graphene sheet which is deposited on glass substrate. The structure supports highly confined THz SPs with weak attenuation. Two laser beams obliquely incident, from free space on the graphene sheet. These laser beams impart oscillatory velocities to electrons and exert a difference frequency ponderomotive force on the free electrons of the graphene film, the latter beats with the carrier density to produce a nonlinear current that excites THz GSPs at difference frequency in graphene. The novelty of this scheme is that this structure is ripple free structure and phase matching condition is satisfied automatically.

In “Surface Plasmon Dispersion Relation in Graphene,” we derive the dispersion relation for graphene plasmons. The “Non-linear Mixing of Two Laser Beams and THz GSP Excitation in Graphene” section is devoted to THz GP excitation by nonlinear mixing, and the “Discussion” section discussed the results.

Surface Plasmon Dispersion Relation in Graphene

Consider a glass substrate of relative permittivity ϵ_d occupying half space $x \leq 0$ (cf. Fig. 1). The region $x > 0$ is free space. A monolayer graphene of conductivity σ_g is deposited on it. The conductivity is a function of thickness and given by

$$\sigma = \sigma_g \delta(x) \quad (1)$$

and the current density in graphene layer may be defined as

$$J_z = \sigma E_z \quad (2)$$

Consider a SPs propagate (Fig. 1) along \hat{z} as with t - z variations as $\exp[-i(\omega t - k_z z)]$. The electric and magnetic fields of the SPs in different regions can be written as

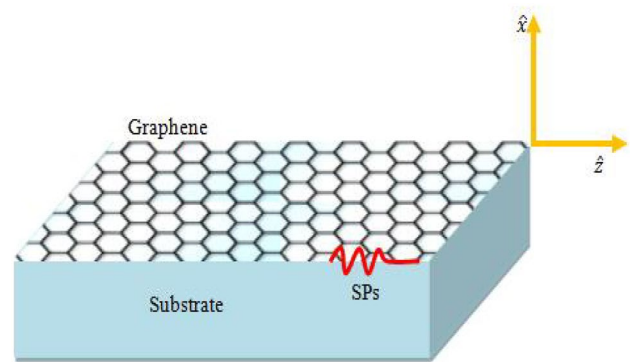


Fig. 1 A monolayer of graphene is deposited on glass substrate

$x > 0$ (Vacuum)

$$\vec{E}(x, z, t) = A(\hat{z} + \frac{ik_z}{\alpha_I} \hat{x}) \exp(-\alpha_I x) \exp[-i(\omega t - k_z \hat{z})] \quad (3)$$

$$\vec{H}_{yI} = \frac{i\omega\epsilon_0}{\alpha_I} \hat{y} A \exp(-\alpha_I x) \exp[-i(\omega t - k_z \hat{z})]$$

$x < 0$ (dielectric)

$$\vec{E}(x, z, t) = A(\hat{z} - \frac{ik_z}{\alpha_{II}} \hat{x}) \exp(\alpha_{II} x) \exp[-i(\omega t - k_z \hat{z})] \quad (4)$$

$$\vec{H}_{yII} = -\frac{i\omega\epsilon_0\epsilon_d}{\alpha_{II}} \hat{y} A \exp(\alpha_{II} x) \exp[-i(\omega t - k_z \hat{z})]$$

where $a_I = (k_z^2 - \omega^2/c^2)^{1/2}$ and $a_{II} = (k_z^2 - (\omega^2/c^2)\epsilon_d)^{1/2}$ are known as the decay constants in free space and dielectric, respectively, [7–9] and k_z is propagation constant of SPs. Using jump condition on \vec{H} at $x = 0$), $\oint \vec{H} \times d\vec{l} = \int \vec{J} \times d\vec{s} + \int \frac{\partial \vec{D}}{\partial t} \times d\vec{s}$ one may get

$$\vec{H}_{yI} - H_{yII} = \sigma_g \int \delta(x) E_z dx$$

$$\vec{H}_{yI} - H_{yII} = \sigma_g E_z|_{x=0} \quad (5)$$

Putting Eqs. (3) and (4) into Eq. (5), one may get

$$\frac{1}{(k_z^2 - \frac{\omega^2}{c^2})^{1/2}} + \frac{\epsilon_d}{(k_z^2 - \frac{\omega^2}{c^2}\epsilon_d)^{1/2}} = \frac{N_0 e^2}{\omega^2 \epsilon_0 m^*} \quad (6)$$

Eq. (8) gives the SP dispersion relation in graphene, where m^* is the effective mass of electron and is given by $m^* = \epsilon_F/v_F^2$, v_F is the Fermi velocity of electron ($\approx 10^8$ cm/sec), and N_0 is the

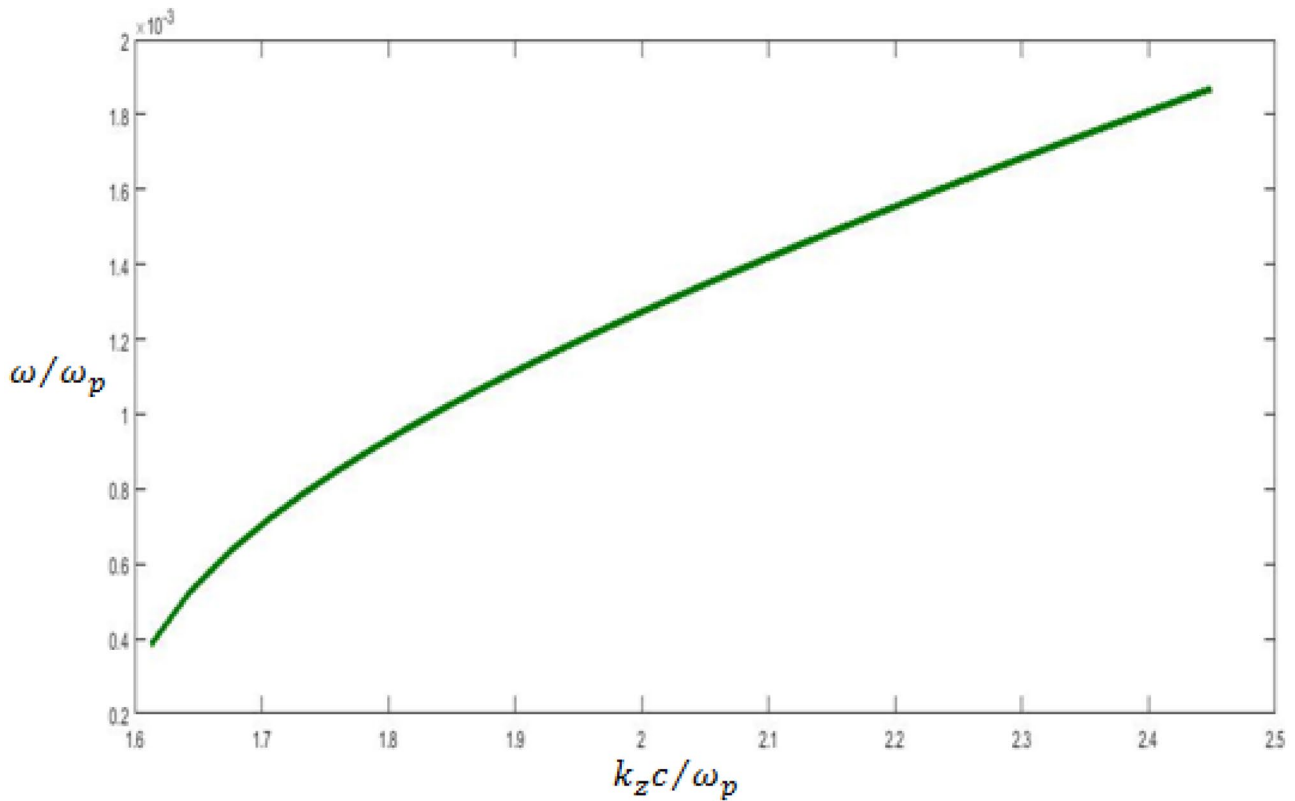


Fig. 2 Dispersion relation of graphene plasmons

free electrons surface density in graphene. In Fig. 2, we have plotted normalized (ω/ω_p) versus normalized ($k_z c/\omega_p$) for the SPs for typical parameters: $v_F/c = 1/300$, $\epsilon_d = 2.5$. The figure shows that at low frequency ω varies linearly with k_z . However, at higher frequencies it varies gradually, because there is a weak coupling between lasers and graphene plasmons.

Non-linear Mixing of Two Laser Beams and THz GSPs Excitation in Graphene

Consider two lasers which are y-polarized and incident on a graphene sheet deposited on a dielectric substrate (cf. Fig. 3), the laser beams may be written as

$$\vec{E}_1 = \hat{y}A_1 \exp[-i(\omega_1 t - k_{1x}\hat{x} - k_{1z}\hat{z})] \tag{7}$$

$$\vec{E}_2 = \hat{y}A_2 \exp[-i(\omega_2 t - k_{2x}\hat{x} - k_{2z}\hat{z})] \tag{8}$$

The phase matching conditions demands that

$$\omega_{SPTHZ} = \omega_1 - \omega_2, k_{SPTHZ} = k_1 - k_2 \tag{9}$$

The lasers impart oscillatory velocities to the electrons, given as

$$\vec{v}_1 = \frac{e\vec{E}_1}{m i \omega_1} T_A, \vec{v}_2 = \frac{e\vec{E}_2}{m i \omega_2} T_A \tag{10}$$

Here, we consider the transmission coefficient of two laser beams being same and taking into account the transmission effect. These laser beams also impart a ponderomotive force on electrons at beat frequency, so the force is given by

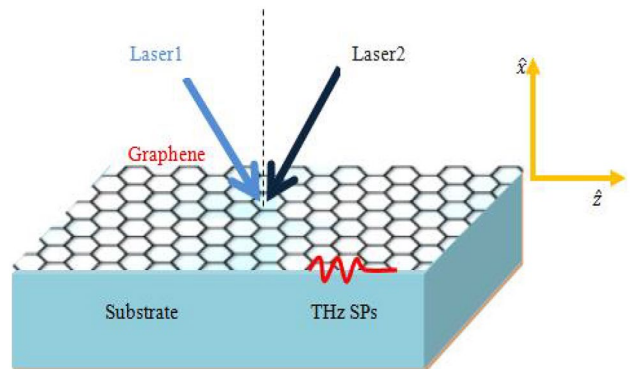


Fig. 3 Two laser beams obliquely incident from free space on the graphene sheet

$$\vec{F}_p = -\frac{e}{2}(\vec{v}_1 \times \vec{B}_2^* + \vec{v}_2^* \times \vec{B}_1) \tag{11}$$

The z component of Eq. (11) may be written as

$$F_{pz} = -\frac{m}{2}i(k_{1z} - k_{2z})\vec{v}_1 \cdot \vec{v}_2^* \tag{12}$$

The ponderomotive force also imparts oscillatory velocity to electrons at frequency $(\omega_1 - \omega_2)$ and may be written as

$$\vec{v}_{(\omega_1 - \omega_2)} = \frac{-\vec{F}_p}{mi(\omega_1 - \omega_2)} \tag{13}$$

the nonlinear current may be written as

$$\vec{J}_\omega^{NL} = -\hat{z}n_0e\frac{(k_{1z} - k_{2z})}{2(\omega_1 - \omega_2)}\vec{v}_1 \cdot \vec{v}_2^* \cong \hat{z}Fd \exp[-i(\omega t - k_{THz}z)]\delta(x) \tag{14}$$

where

$$F = -n_0^0e\frac{(k_{1z} - k_{2z})}{4\omega}\frac{e^2A_1A_2}{m^2\omega_1\omega_2}|T_A|^2 \tag{15}$$

$$\frac{A_0}{A_1} = \frac{1}{(\omega/\omega_p)}\left(\frac{\omega}{4\omega_1}\right)\left(\frac{k_{1z} - k_{2z}}{k_z}\right)\frac{|v_2|}{c}|T_A|^2\frac{(d\omega_p/c)(L\omega/c)}{1/(k_z^2c^2/\omega^2 - 1)^{3/2} + \epsilon_d/(k_z^2c^2/\omega^2 - \epsilon_d)^{3/2}} \tag{23}$$

where $T_A = 2/1 + \frac{\epsilon_g(\omega/c)\cos\theta_i}{k_{1-THz}}$ is transmission coefficient, $k_{1-THz} = \sqrt{\frac{\omega^2}{c^2}\epsilon_g - \frac{\omega^2}{c^2}\sin^2\theta_i}$. The nonlinear current density manifests itself in the jump condition on \vec{H}_y of the SPs, i.e.,

$$H_y|_{x=0^+} - H_y|_{x=0^-} = \sigma_g dE_z|_{x=0} + Fd \exp[-i(\omega t - k_{THz}z)] \tag{16}$$

Substituting Eqs. (3) and (4) into Eq. (16), we get

$$\left\{\frac{1}{\alpha_l} + \frac{\epsilon_d}{\alpha_{II}} + \frac{\sigma_g d}{i\omega\epsilon_0}\right\}A = \frac{Fd}{i\omega\epsilon_0} \cong -i\frac{Fd}{\omega\epsilon_0} \tag{17}$$

Equation (17) can be written as

$$DA = -i\frac{Fd}{\omega\epsilon_0} \tag{18}$$

where

$$\frac{1}{\alpha_l} + \frac{\epsilon_d}{\alpha_{II}} + \frac{\sigma_g d}{i\omega\epsilon_0} = D \tag{19}$$

At exact phase matching D vanishes. However, due to finite length of interaction $L = 2r_0$ where $r_0 =$ laser spot size so D can be replaced by region $D \cong -i(\partial D/\partial k_z)(\partial/\partial z)$, Eq. (19) can be written as

$$\frac{\partial D}{\partial k_z} = -k_z\left(\frac{1}{\left(k_z^2 - \frac{\omega^2}{c^2}\right)^{3/2}} + \frac{\epsilon_d}{\left(k_z^2 - \frac{\omega^2}{c^2}\epsilon_d\right)^{3/2}}\right) \tag{20}$$

If there is free electron collision, the SP has a finite imaginary part in $k_z, k_z = k_{zr} + ik_{zi}$, and $D \cong -i(\partial D/\partial k_z)(\partial/\partial z + k_i)$, putting in Eq. (18), one may get

$$\frac{\partial A_0}{\partial z} + k_i A_0 = \frac{Fd/\omega\epsilon_0}{\partial D/\partial k_z} \tag{21}$$

For interaction length $L \approx 2r_0 > 1/k_i$ (attenuation length), $A_0 = (Fd/\omega\epsilon_0)/k_i(\partial D/\partial k_z)$ and for interaction length $L < 1/k_i$ (attenuation length) $A_0 = (FdL/\omega\epsilon_0)/(\partial D/\partial k_z)$, we get

$$A_0 = \frac{n_0^0e}{4\omega}(k_{1z} - k_{2z})\frac{e^2A_1A_2}{m^2\omega_1\omega_2}|T_A|^2\frac{dL}{\omega\epsilon_0\left\{k_z\left(1/\alpha_l^{3/2} + \epsilon_d/\alpha_{II}^{3/2}\right)\right\}} \tag{22}$$

Solving and rearranging the terms in Eq. (22), we get

Equation (23) gives the ratio of terahertz graphene plasmons to the amplitude of laser beam, where v_2 is the oscillatory velocity of electron, c is the speed of light, ω and ω_1 are the frequencies of incident laser beams, $d\omega_p/c$ is the normalized thickness, and $L\omega/c$ is the normalized length of interaction. We have plotted Eq. (23) for the following parameters corresponding to modest laser intensity $\sim 10^{12}$ W/cm² at 1 μ m wavelength [19]: $v_2 = 10^6$ m/s, $c = 3 \times 10^8$ m/s, $\epsilon_d = 2.5$, $k_z^2c^2/\omega^2 = 2.6$, $\omega \approx 10^{13}$ rad/s, $\omega_1 \approx 2 \times 10^{12}$ rad/s, $\omega_p \approx 2.5 \times 10^{12}$ rad/s, $d\omega_p/c \approx 10^{-2}$, $L\omega/c \approx 10$, and $|T_A| \approx 97\%$. As the terahertz frequency and thickness are raised, the amplitude falls monotonically (cf. Fig. 4) because at higher frequency and large thickness, the coupling between graphene SPs and laser is weak.

Discussion

In the conclusion, we studied the promise of producing THz SPs at difference frequency in graphene sheet by using nonlinear mixing of two laser beams, which have frequency difference in THz range at modest power lasers. The nonlinearity arises through the ponderomotive force. The THz SPs are strongly localized near around the graphene sheet and propagate at long distance

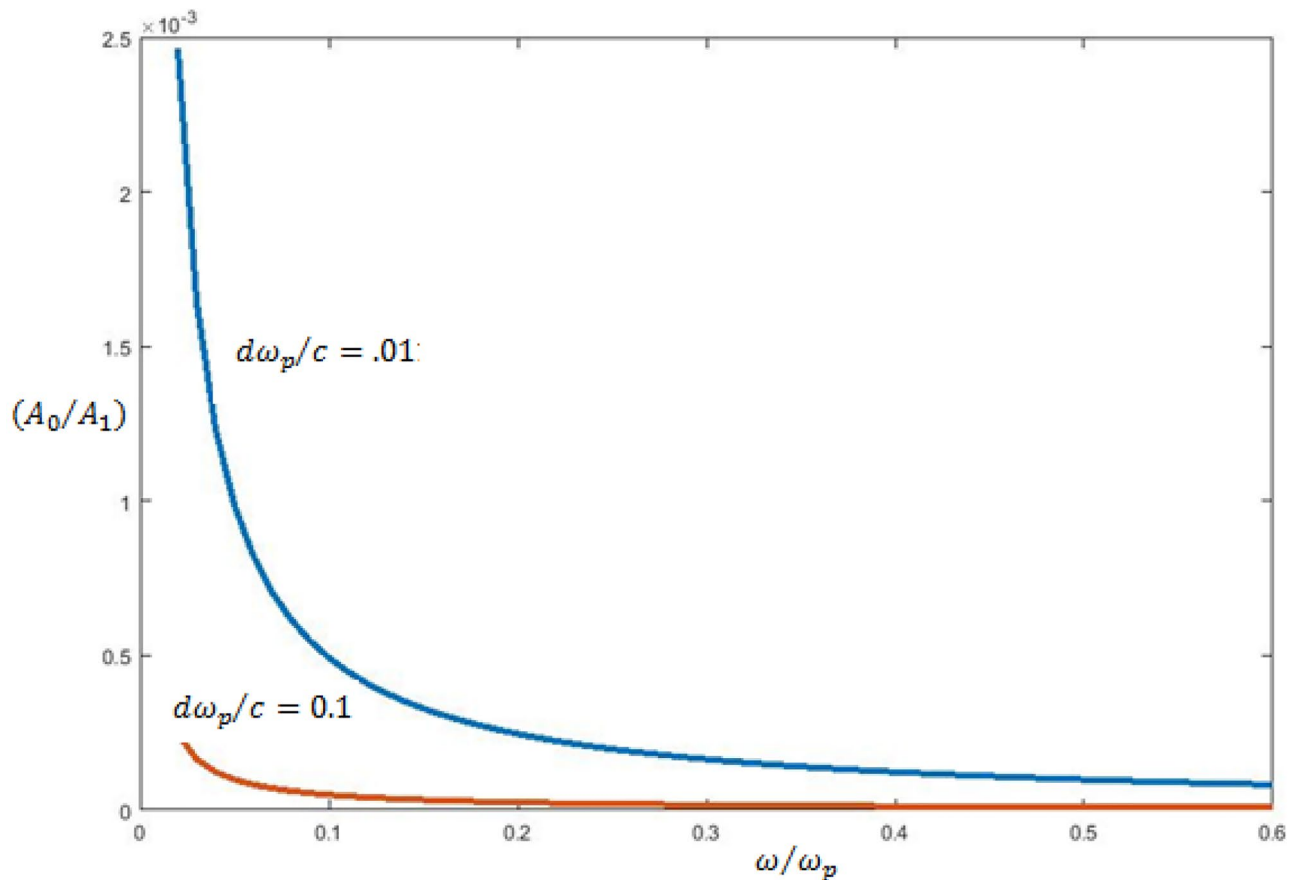


Fig. 4 Normalized THz SP amplitude variation with normalized frequency for two different normalized thickness

along the interface. The attenuation of THz SP in graphene is weak because they are highly localized and efficiently excited by modest laser power $\sim 10^{12}$ W/cm². The ratio of THz SP field amplitude and laser amplitude is of the order $\sim 10^{-4}$ at laser intensity $\sim 10^{12}$ W/cm² at $1 \sim \mu\text{m}$ wavelength. The efficiency has been upper bound given by Manley -Rowe relations. This scheme will be useful for making the THz radiation source for future applications.

Authors' Contributions All authors contributed equally to this work.

Data Availability The data that supports the findings of this study are available within the article.

References

- Neto AC, Guinea F, Peres N, Novoselov KS, Geim AK (2009) Rev Mod Phys 81:109
- Novoselov K, Geim AK, Morozov S, Jiang D, Katsnelson M, Grigorieva I, Dubonos S, Firsov A (2005) Nature 438:197
- Horng J, Chen C-F, Geng B, Girit C, Zhang Y, Hao Z, Bechtel HA, Martin M, Zettl A, Crommie MF et al (2011) Phys Rev B 83:165113
- Liu M, Yin X, Ulin-Avila E, Geng B, Zentgraf T, Ju L, Wang F, Zhang X (2011) Nature 474:64
- Ju L, Geng B, Horng J, Girit C, Martin M, Hao Z, Bechtel HA, Liang X, Zettl A, Shen YR et al (2011) Nat Nanotechnol 6:630
- Vakil A, Engheta N (2011) Science 332:1291
- Raether H (1988) Surface plasmons on smooth and rough surfaces and on gratings. Springer, Berlin
- Boardman AD (1982) Electromagnetic surface modes. Wiley, New York
- Maier SA (2007) Plasmonics: Fundamentals and applications. Springer-Verlag, New York
- Barnes WL (2003) Alain Dereux and Thomas W. Ebbesen, Nature 424:824
- Liu S, Zhang P, Liu W, Gong S, Zhong R, Zhang Y, Hu M (2012) Phys Rev Lett 109:153902
- Hwang E, Sarma S (2007) Phys Rev B 75:205418
- Jablan M, Buljan H, Soljagic M (2009) Phys Rev B 80:245435
- Grigorenko AN, Polini M, Novoselov KS (2012) Nature Photon 6:749
- Wong LJ, Kaminer I, Ilic O, Joannopoulos JD, Soljačić M (2016) Nat Photonics 10:46
- Liu S, Zhang C, Hu M, Chen X, Zhang P, Gong S, Zhao T, Zhong R (2014) Appl Phys Lett 104:201104

17. Constant TJ, Hornett SM, Chang DE, Hendry E (2015) *Nat Phys* 12:124
18. Yao B, Liu Y, Huang S-W, Choi C, Xie Z, Flores JF, Wu Y, Yu M, Kwong D-L, Huang Y, Rao Y, Duan X, Wong CW (2018) *Nat Photon* 12:22
19. Pawan Kumar and V.K.Tripathi, *J. Appl. Phys.* 114, 053101 (2013).
20. Prashant Nagpal, Nathan C. Lindquist, Sang-Hyun Oh, David J. Norris, *Science* Vol. 325, Issue 5940, 594(2009)
21. Ryzhii M, Ryzhii V (2007) *Jpn J Appl Phys, Part 2* 46:L151
22. Watanabe T, Fukushima T, Yabe Y, Tombet SAB, Satou A, Dubinov AA, Aleshkin VY, Mitin V, Ryzhii V, Otsuji T (2013) *New J Phys* 15:075003
23. Tantiwanichapan K, DiMaria J, Melo SN, Paiella R (2013) *Nanotechnology* 24:375205